The American University in Cairo
الجامعة الأمريكية بالقاهرة

Graduate Studies

Development of an Electromagnetic System for Wireless Magnetic Manipulation of Soft Capsule Endoscope for Drug Delivery Applications

A THESIS SUBMITTED BY

Nada Ashraf Hussein Mahmoud

TO THE

The Department of Mechanical Engineering

SUPERVISED BY

Prof. Mohamed Serry
Professor, Department of Mechanical Engineering
The American University in Cairo

Dr. Islam Khalil
Assistant Professor, Department of Biomechanical Engineering
The University of Twente

September 4, 2023

in partial fulfillment of the requirements for the degree of
Master of Science in Mechanical Engineering

Declaration of Authorship

I, Nada Ashraf Hussein declare that this thesis titled, "[Thesis title]" and the work presented in it are my own. I confirm that:

- This work was done wholly or mainly while in candidature for a research degree at thisUniversity.
- Where any part of this thesis has previously been submitted for a degree or any otherqualification at this University or any other institution, this has been clearly stated.
- Where I have consulted the published work of others, this is always clearly attributed.
- Where I have quoted from the work of others, the source is always given. With the exception of such quotations, this thesis is entirely my own work.
- I have acknowledged all main sources of help.
- Where the thesis is based on work done by myself jointly with others, I have made clearexactly what was done by others and what I have contributed myself.

Signed:

Nada Ashraf

Date:
September 2023

Abstract:

Wireless capsule endoscopy (WCE) is a remarkable diagnostic device that examines the gastrointestinal (GI) tract. The WCE is a small capsule integrated with a camera that is used to visualize the inner mucosa of the GI tract. WCE has been proven to be the most effective method to diagnose GI diseases and GI cancers. The procedure reduces the discomfort and risk compared to conventional endoscopy methods. However, current WCEs lack the ability to take a biopsy or deliver a drug to a specific location. Those therapeutic functions can be introduced by wirelessly controlled WCEs.

This thesis introduces an electromagnetic system that uses a magnetic field to wirelessly maneuver the capsule inside the GI tract. An enhanced control method for controlling the steering of the capsule endoscope is presented. The control method uses image processing feedback to enhance the controllability of the WCE and enlarge the effective workspace. The final constructed system consists of 8 electromagnetic coils and can steer the capsule in the x-y plane. Additionally, a novel design of an untethered capsule endoscope that can deliver a drug to a specific location inside the GI tract wirelessly is presented. In conclusion, we present an electromagnetic system that enhances the controllability and therapeutic functions of the WCEs.

Acknowledgment:

I would like to thank my parents, Ashraf Hussein and Ghada Mohamed for their endless love and support. No words can describe my gratitude for their patience and support. Also, I would like to thank my advisor, Prof. Mohamed Serry for giving me the opportunity to enhance my skills and supporting me with many resources during my master's journey. I thank my co-advisor, Dr Islam Khalil for his support and knowledge. I would like to thank my lab teammates, Eslam El Gamal, Omar Ibrahim, and Yousef Kotb for their time and efforts in supporting me. This Thesis is partially funded by the American University of Cairo.

Contents:

List of Figures:

List of Tables:

List of Symbols:

T	Magnetic torque
m	Magnetic dipole moment
B	Magnetic field
F	Magnetic force
∇	Gradient
I	Electric current
$\tilde{B}$	Unit current magnetic field

Chapter 1 Introduction

1.1 Motivation

Cancer is a serious disease that threatens the entire world and is the second leading cause of mortality. In the United States, there were 609,360 cancer deaths and about 1.9 million new cancer diagnoses in 2022[1]. The digestive system cancer cases are almost 32% of all cancer deaths[1]. Over the past 80 years, there have been great efforts to find answers to this devastating crisis that resulted in great improvements in the early detection and treatment of cancer which helped in reducing mortality rates[2]. However, to increase early cancer detection and treatment effectiveness, additional research must be done in order to reduce treatment side effects. Current chemotherapeutic cancer treatments are less effective because the anti-cancer drugs slowly reach the tumor cells that are distant from blood vessels [3], [4]. The low selectivity (tumor targeting) of anti-cancer drugs is another deficiency that results in systemic exposure of healthy cells to anti-cancer drugs. Chemotherapy can be enhanced through better anti-cancer drug cargo targeting tumor cells.

Endoscopic technology has been the main tool for visualizing and diagnosis of gastrointestinal (GI) tract cancers. The traditional flexible endoscope has improved significantly over the last 200 years [5]. The endoscope has become more flexible and accurate using enhanced flexible materials; in addition to, using high-definition cameras instead of using mirrors. These developments help in making the diagnostic procedure less painful and increase the accuracy of the diagnosis. However, it still causes pain and discomfort to patients and usually, it requires sedation for the patients. All these challenges paved the way for introducing new technology to ease the pain and discomfort that results from the traditional endoscopy.

In 2000, a wireless capsule endoscope (WCE) was introduced for diagnosing GI diseases, because it can be easily swallowed by patients due to its small size, then capture

images of the GI tract for diagnosis[6]. Because of its small size, WCEs have minimized the discomfort, pain, and risk of the endoscopic procedure. Moreover, it succeeded in taking visual images of the small intestine, which was very difficult using traditional endoscopes. However, WCEs have some challenges and limitations, such as lack of controllability. Current commercially available WCEs are moving through the GI tract by natural peristalses and cannot be controlled. This challenge limits the capabilities that can be offered by WCEs. Doctors still use traditional endoscopes if they need to further examine suspicious cells, take a biopsy, or deliver drugs. While wireless capsule endoscopy is already used in the clinic to improve the diagnosis of GI tract diseases, the capabilities that can be offered by wireless capsule endoscopy are still being investigated. The WCE can be enhanced to take a biopsy or deliver the drug to a selective area, making it one of the promising technologies that can improve early detection and cancer treatment efficiency.

The focus of this research study is the development of an electromagnetic system that can wirelessly control soft capsule endoscopes. It is expected to have great capabilities in bioengineering applications, especially targeted drug delivery systems. Advanced drug delivery systems are more adequate than the current traditional ones, as they can deliver a drug to a selected site, more easily and accurately which leads to less needed doses and reduces the painful side effects of the treatment. Such capabilities make wirelessly controlled capsule endoscopy a valuable step towards more efficient targeted drug delivery systems.

1.2 Outline of the Thesis

This thesis is structured as follows, background of wireless capsule endoscope technology and literature review are introduced in Chapter 2. Then in Chapter 3, the theoretical foundation and theory behind the control algorithm are presented. Followed by the methodology and experimental work, manufacturing the actuation system, and fabricating the capsule endoscope are illustrated in Chapter 4. Next, the results of the experiment conducted as a proof of concept and discussion of the results are presented in Chapter 5. Finally, the conclusion of the thesis is presented in Chapter 6.

Chapter 2 Review of the Literature:

Gastrointestinal (GI) cancers are considered one of the most common cancers with a high mortality rate[1]. Early diagnosis has a significant effect on curing cancers, as the early diagnosis survival rate can reach 90% while it is reduced to below 20% for late diagnosis[7]. One of the main tools that is used for GI diseases/cancer diagnosis is GI endoscopy. Philipp Bozzini was the pioneer of developing endoscopy in the early years of the 1800s [8]. In 1822, William Beaumont, an army surgeon, proposed the idea of using endoscopy to examine the human GI tract. The majority of endoscopic techniques used up until the end of the 1990s were based on the flexible tube[9].

The diagnosis of numerous diseases was previously only possible in the upper 1.2 meters and lower 1.8 meters of the colon and rectum of the GI tract, using gastroscopy and colonoscopy[9]. The process was unable to adequately identify the type of disease and the precise GI tract regions that were infected. Additionally, the treatment is time-consuming and requires the use of a large-diameter tube, making it challenging to complete and causing the patient's discomfort and pain. Often this procedure requires sedation as it requires inserting the endoscope through the mouth or the anus into the digestive system. Moreover, the traditional endoscopy cannot reach the entire small intestine. These challenges paved the way for the development of a wireless capsule endoscope.

The idea of embedding a tiny camera in a pill for human GI tract imaging was first introduced by Iddan et al. in 1981[10], and it was later developed and became a prototype of the WCE in 1997 [11]. The first WCE system, called M2A™ (Figure 2.1), was commercialized by "Given Imaging" in 2000 [12]. With the ability to monitor the whole length of the GI tract, the WCE marked a turning point in the development of endoscopy. However, doctors still use

traditional endoscopes if they need to inspect certain areas or take a biopsy. That demand revealed further challenges in controlling the location of WCE.

Figure 2-1 M2A^{TM} Capsule (a) and schematic diagram of its components (b): optical dome (1), lens holder (2), short focal length lens (3), four LEDs (4), CMOS image sensor (5), two silver oxide batteries (6), ASIC radio-frequency transmitter (7) and external receiving antenna (8) – Retrieved from [12]

Modern robots and conventional diagnostic technologies can be used to enhance the mobility and controllability of the WCEs, which may offer innovative answers to the aforementioned issues. For this goal, many actuation techniques and energy sources have been investigated, such as pneumatic or hydraulic [13]–[15], electromechanical [16]–[18], hybrid [19], [20], and magnetic methods [21], [22]. The features of the other examined actuation methods, however, are far from optimal in comparison to magnetic actuation. For instance, electromechanical and pneumatic or hydraulic are difficult to design, and the commonly prescribed driving processes could result in extensive intestinal injuries and considered expensive. On the other hand, magnetic actuation systems use an external magnetic field to maneuver and control medical devices to perform a diversity of diagnoses and treatments. In comparison to mechanical systems, magnetic actuation systems allow for remote manipulation of devices and the penetration of body flesh without injuring the intestinal organs. As a result, medical applications of magnetic actuation systems are considered less risky. Permanent magnets and electromagnetic coils are the two main methods of producing magnetic fields. The

first application of permanent magnets in medicine was for the extraction of metal parts from the human body. In 1951, permanent magnets were used to show how to control a catheter inside an animal's abdominal aorta [23]. In the 2000s, a magnetic actuation system consisting of six electromagnetic coils was proposed to control a catheter for brain biopsy [24]. The first magnetic actuation system for magnetic catheter guidance, that was clinically authorized, was released to the market by Stereotaxis in 2003. After cardiovascular procedures, magnetic actuation technology was used in ophthalmic, neuro, and drug delivery procedures [25]–[29]. Since its use in 2006 to examine the GI tract, the technique has gradually gained popularity among researchers in the field of medicine [30]. Extensive studies have been conducted to develop magnetic actuation technology. Several businesses have already started using magnetic actuation capsule endoscopes for commercial purposes in the abdomen [31]. A magnetic actuation system generates controlled magnetic fields to maneuver the capsule endoscope. According to the method of generating the magnetic field, the magnetic actuation systems are divided into two main categories: moving permanent magnet systems, and stationary electromagnetic systems.

2.1 Moving Permanent Magnet Systems:

Controlling a capsule endoscope (CE) with a rotating external magnet was introduced by Carpi et al. in 2007 [32]. They added magnetic particles to the M2A capsule (Figure 2-1) to be controlled by the magnetic field. Permanent magnets were part of the external control device, and they generated a magnetic field that was used to navigate and rotate the capsule endoscope on the inner mucosa of the tissue. This preliminary analysis was the first step toward the development of magnetic actuation capsule endoscopes.

In 2010, Valdastri et al. [33] controlled a capsule (diameter: 15 mm; length: 48 mm; weight: 14.4 g) with an external magnet (diameter: 60 mm; Length: 70 mm; weight: 1500 g).

Similar to an ultrasound machine, the device's magnet was mounted on hydraulic arms and was operated by a doctor. The capsule endoscope had a transmission system that consisted of a motor and worm gear. The gear moved the magnet inside the capsule in response to the motor's rotational motion, rotating both the magnet and the casing. This reduced the load on the doctor by enabling the capsule to be adjusted depending on the surrounding tissue without moving the external magnet. By conducting in vivo tests on a deceased pig, a 360° panoramic view of the abdomen was produced to evaluate the controlling capability of the capsule endoscope. However, the capsule can show only a 45° view of the colon due to contact with the side wall.

Pittiglio et al presented a magnetic actuation system that controls and levitates a magnetic flexible endoscope using a single permanent magnet that is controlled by a robotic arm (KUKA Med) in 2019 [34], [35]. As shown in Figure 2.2a, the system was used to levitate a flexible endoscope inside the colon. The levitation helps reduce the pressure and friction against the bowel wall, which reduces patient pain and discomfort. Although this system was used to control the flexible endoscope, it can be used to control wireless capsule endoscope. In 2013, the Mirocam-Navi system was created by IntroMedic Co., Ltd. [39]. The magnet has the following characteristics: 260 mm in length, 35 mm in handle width, 65 mm in head width, 0.5 T of magnetic field, and 2.63 N of magnetic force on the capsule. The system has proven a comparable diagnostic rate to traditional flexible endoscopy through 26 human stomach studies [36]. The OMON MACE and the InsightEyes EGD system were created by Lin et al. [37] and have been effectively used in hospitals as a physical diagnostic device. A system for guiding magnetic actuation flexible endoscopes was initially introduced by Ciuti et al. [38], [39]. The system moved the flexible endoscope inside the GI tract using a permanent magnet controlled by a 6-DOF robotic system that could navigate the capsule along the body.

In 2011, Mahoney et al [40], [41] proposed to use a permanent magnet actuation system to control a screw-shaped capsule endoscope by regularly rotating along a fixed axis. The

model consists of a 6-DOF robotic arm, an extra motor, and a NdFeB magnet. The motor rotates the magnet, while the robotic arm handles its position and orientation. At every location in the working space, an equivalent magnetic field vector is produced as the magnet spins around a fixed axis. The magnetic robot rotates constantly because of the magnetic field vector's simultaneous rotation around its fixed axis. In vitro studies, the technology demonstrated promising results with magnetic robots including spiral and rolling ball robots [41], [42]. The model, which makes use of a single permanent magnet, is nonetheless frequently affected by an unwanted force of attraction between the magnetic robot and the magnetic actuation system. Deformation and possible harm to the GI tract may be caused if the force is not controlled. The stepping motion of the magnet can also become out of phase with the rotating magnetic field or possibly lose it totally with just a slight variation in friction. Mahoney et al developed a magnetic force control technique to address these problems, in which, six linear magnetic sensors were utilized to monitor the magnetic field, allowing closed-loop control to minimize the overshoot angle and prevent the capsule's loss [43], [44].

In 2013, Arezzo et al [45] added a 1-DOF device to the end of the original 6-DOF robotic arm to expand the robot's flexibility to achieve the entire capabilities needed for operating with the endoscope. An NdFeB permanent was attached to the end-effector of the 7-DOF robotic arm. During the procedure, a gyroscope was placed inside the endoscope to avoid its loss. This made it possible to identify the loss of the flexible endoscope, which would be signaled by an alarm. Moreover, they added an algorithm to continuously observe the amplitude of the magnetic flux. The experiments proved that the magnetic actuation of flexible endoscopes was feasible and that it was sufficiently accurate when compared to traditional flexible endoscopy. In 2016, Mahoney et al [46] improved a magnetic actuated system utilizing a commercial 6-DOF robotic arm with a permanent magnet attached to its end-effector. The system achieves 3-DOF closed loop directional control and 2-DOF open loop rotation control

by using direct actuation of magnetic force and torque to control the capsule endoscope. The limitation of kinematic singularity and joints of the manipulator were the key research areas. By giving up the capsule's direction control authority when the permanent magnet attached to the end-effector of the robotic arm enters a kinematic singularity enables the system to keep control of the capsule's 3-DOF position. The feedback for the closed-loop 3-DOF control is provided by two cameras to calculate the capsule's position (the orientation is not determined).

A spherical magnetic actuation system, known as the SAMM, was developed in 2017 by Chaluvadi et al to enhance the resolution of kinematic singularity constraints in the magnetic actuation system [47], [48]. Using three omnidirectional wheels, the SAMM achieves omnidirectional control of a spherical permanent magnet and allows it to continually spin around any axis, As shown in Figure 2.2d. For determining the direction of the magnetic dipoles of the permanent magnet, the SAMM also includes a magnetic field sensor system. Design-wise, SAMM is free of kinematic singularities and joint restrictions, allowing the use of robots with less than six degrees of freedom in magnetic actuation systems. The SAMM has demonstrated good performance and ability to provide continuous rotational and directional control of magnetic force and torque. Moreover, the magnetic actuated micro-robot swarms can be controlled by the alternating magnetic dipole field produced by the SAMM [49].

In 2019, Jiang et al [50] introduced a magnetic actuation system, which includes a C-arm type robotic manipulation arm, a capsule endoscope, a localization system for the capsule, and a data recorder, as shown in Figure 2.2b. The single spherical permanent magnet head and C-arm robot have a combined 5-DOF in a working space of 50 x 50 x 50 cm, the maximum adjustable magnetic field is 200 mT. The system's accuracy is comparable to traditional flexible endoscopy and is mostly applied for stomach magnetic control examinations [51]. The device contains a robotic arm with a magnet attached to its end-effector that can move the capsule endoscope in all directions at 300 mm. The system can produce a magnetic field of (200±50)

mT. Because the robotic arm is housed inside the system, there may be fewer safety concerns when patients are close to moving machinery. The system exhibits comparable diagnostic outcomes to traditional flexible endoscopy, with a 94.41 % overall agreement [52]. Cheng et al developed a standing magnetic actuation capsule endoscope system that resembles an X-ray machine for the chest backplane to increase system safety [53].

In 2021, a magnetic actuation colonoscopy system with a servo motor and permanent magnet operated by a belt was proposed by Yen et al. [54]. The device, shown in Figure 2.2c, has a working space of 65 x 65 x 41 cm. The image processing-based object identification and orientation control system achieves semi-automatic manipulation control that can moderate inspection time. The deep learning algorithms used to train the detection model demonstrated great accuracy in each validation metric.

The first in vivo human study using an external magnet was carried out in 2010 by Swain et al. [55]. The system consists of a pair of powerful permanent magnets (10 x 10 x 3 cm) that are housed together in a casing with a handle and weight combined 2.96 kg. A permanent magnet was used in place of the image module in the commercially available capsule endoscope (PillCam), and a temperature-activated switch was used in place of the magnetron switch. This was changed in the following generation to a radio frequency activation technique. The work by Swain et al. showed that CEs could be applied to volunteers' stomachs in a secure and efficient manner [56]. It was challenging for the system to control the vertical movement of the capsule in the esophagus, due to issues including lack of required force and controllability [57].

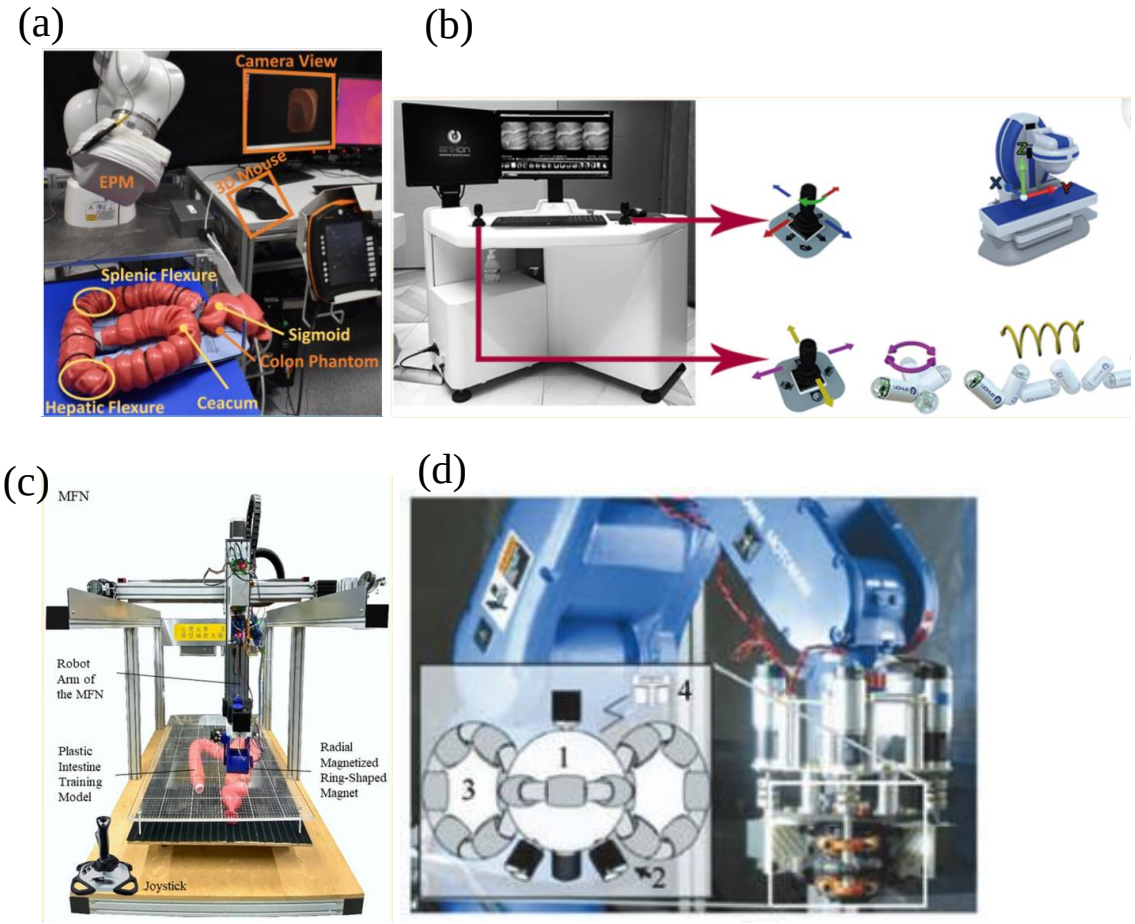

Figure 2-2 Moving Permanent Magnet Systems, a) magnetic levitation system (Pittiglio et al [34]), b) The MCE system (Jiang et al [50]), c) Magnetic actuation with servo motor and permanent magnet (Yen et al [54]), d) Spherical magnetic actuation system (SAMM) (Chaluvadi et al [49])

2.2 Stationary Electromagnetic Systems:

By combining different kinds of coils, such as solenoidal coils, Helmholtz coils, and Maxwell coils, the electromagnetic actuation systems produce magnetic fields. Maxwell coils can produce gradient magnetic fields; however, Helmholtz coils can produce constant magnetic fields. Hence, a gradient field and a 3D uniform magnetic field can be produced by superimposing three Helmholtz coils and three Maxwell coils [58].

In 2010, Kummer et al [59], presented OctoMag, which is a 5-DOF wireless magnetic manipulation system. The system consisted of eight electromagnetic coils to control microrobots wirelessly, as illustrated in Figure 2.3a. Kummer et al introduced the theory of individual decoupling field contribution, which states that if we assume using ideal soft magnetic cores inside the coils, we can assume that the field contributions of the coils are decoupled and can be linearly superimposed. The system was designed for eye operations, however, the same concept was used for controlling other microrobots and capsule endoscopes in later studies [20], [60]. In 2010, Jeon et al. [61], [62] proposed a magnetic actuation system, known as MNS, for controlling capsule endoscope inside blood vessels which consists of 10 coils; six orthogonal Helmholtz coils and saddle coils are used for directional control and the other four coils are Maxwell coils that generate gradient magnetic fields to control the propulsion of the capsule, as illustrated in Figure 2.3b. A magnetic actuation system with eight electromagnetic coils was developed by Hoang et al. [63] to solve the issue of poor driving force and complex coil design used in GI tract inspection. The system has two pairs of rectangular coils, two pairs of Maxwell coils, and a pair of Helmholtz coils; thus, it achieves 3D directional control with fewer coils and maximizes the usage of the workspace, producing 225 mN force.

Keller et al introduced a magnetic actuation system that generates a low magnetic field of 3-10 mT [64]. The system resembles traditional MRI equipment in shape but does not have a cooling system. It comprises six pairs of electromagnetic coils, with a working space of 1 m by 2 m. It was demonstrated through in vivo clinical studies including 53 patients that the system can control the capsule endoscopy in 5-DOF. Clinical research was conducted, including analysis of movement functions (straight, rotate, tilt, etc.) and operator-specific evaluation of each participant. These movements were found to be enough for accessing the entire stomach and obtaining up-close pictures of the gastric mucosa [65]. In 2016, five animal cases of cardiac surgery experiments were conducted using a catheter magnetic navigation system, demonstrating the reliability of the system [66].

In 2019, an electromagnetic system for accurate control of the capsule endoscopy was proposed by Son et al. [67], as shown in Figure 2.3c. The model consists of 9 electromagnets and an array of 64 Hall effect magnetic sensors. The magnetic sensor array is placed on the top and all 9 coils are placed on the bottom of the working area, with enough space between them to prevent saturation of the magnetic sensors. To control the capsule, magnetic gradients in the x-y-z directions are produced by optimizing the magnetic energy well. The hall-effect sensors array calculates the position of the capsule by applying an algorithm that subtracts the contribution of the electromagnet's magnetic field from the recorded magnetic field and performs a nonlinear optimization to determine the position of the capsule in real time [68]. As a result, this system's active control of capsule endoscopy and sensor array localization system have contributed to accurate inspection of the stomach [67].

Figure 2-3 Stationary Electromagnetic Systems, a) The OctoMag (Kummer et al[59]), b) The MNS system (Jeon et al [61]), c) Nine-coil electromagnetic system (Son et al [67]), d) The MNCE system (Sun et al [69]).

In 2022, Sun et al [69] carried out a study on an enhanced and upgraded magnetic actuation system, known as the MNCE system, to diagnose the entire GI tract, as shown in Figure 2.3d. Three fundamental control strategies were proposed to adapt to the complicated GI tract environment, and their viability was originally examined utilizing experiments on a 3D-printed model. In vivo experiments were conducted in 2022 [70]. This demonstrates an enhanced and integrated magnetic actuation system that could examine the esophagus, stomach, and colorectum all at once. X-ray image analysis and anatomical investigations were used to further show the system's effectiveness and safety.

Safety is the main advantage of the stationary electromagnetic system compared to the moving permanent magnet systems. Although permanent magnet systems can generate stronger magnetic fields with less heat produced and energy usage, electromagnetic systems are considered safer as they can be switched off immediately in case of emergencies. However, the permeant magnets cannot be demagnetized. Another advantage of electromagnetic systems is generating variable magnetic fields and magnetic gradients without the need to move any part of the system. Moreover, they can diagnose and inspect many parts of the GI tract. The electromagnetic system can extend the application of capsule endoscope technologies to the cardiovascular system and GI tract and has higher application scalability than permanent magnet systems.

2.3 Research Aim:

Based on the literature review, the Capsule endoscope has improved radically, from the original handheld endoscope, introduced in 1822 to the existing wireless capsule endoscope (WCE). Wireless capsule endoscope is considered the main method to diagnose GI tract diseases because it improves the accuracy of the diagnosis, makes the procedure much less painful, and lowers the risk of fatal mistakes. Modern studies still explore the possibilities afforded by WCE [71]. The inability of commercially available WCEs to deliver a drug to a specific location inside the GI tract is one of their main limitations. Another limitation of the WCE is the lack of controllability, since the current commercially available WCEs are passively actuated by GI tract peristalses, and they cannot be controlled by a doctor directly. These two limitations triggered a new research area.

The aim of this thesis is to improve the diagnostic accuracy and therapeutic potential of the WCEs by addressing the above-mentioned limitations. To improve the controllability of the WCE, remote manipulation methods must be enhanced. Moreover, the WCE's design significantly affects the diagnostic accuracy and their ability to deliver drugs wirelessly, therefore, design improvement must be considered.

Our main study area is a magnetically actuated capsule endoscope since it has advantages over other actuation methods for capsules, as we have already illustrated in the previous section. We use magnetically actuated soft capsule endoscopes in particular because of their potential application in cutting-edge therapeutic activities. [67], [72]–[74]. Moreover, we chose an electromagnetic actuation system due to its ability to manipulate objects at a distance and penetrate the human flesh without causing injury to the patient.

In conclusion, the final goal of this research is to develop a magnetically automated system that can conduct a visual endoscopy and deliver drugs under the supervision of a medical operator. Hence the main objectives of the thesis are:

- Develop an electromagnetic actuation system to enhance the manipulation and controllability of the WCE.
- Improve the actuation algorithms by introducing image processing position feedback.
- Increase the diagnostic accuracy and ability to deliver drugs to a specific location wirelessly using AC induction heating.

Chapter 3 Theoretical Background:

The magnetic torque and force, applied on a magnet placed in the magnetic field B, can be calculated below:

$$T = m \times \mathrm{B} \qquad (3.1)$$

$$F = (m \cdot \nabla)\mathrm{B} \quad (3.2)$$

Where T is the magnetic torque, F is the magnetic force and m is the magnetic dipole moment of the magnet [75]. Maxwell's equation states the below constraint in equation (3.3) since there is no current produced in the working space.

$$\nabla \times B = 0 \qquad (3.3)$$

By using the skew-symmetric matrix form to represent the vector cross-product, eq. (3.1) can be represented by below:

$$T = \begin{bmatrix} 0 & -m_z & m_y \\ m_z & 0 & -m_x \\ -m_y & m_x & 0 \end{bmatrix} \begin{bmatrix} B_x \\ B_y \\ B_z \end{bmatrix} \qquad (3.4)$$

According to Petruska et al. [76], the spatial derivative of the magnetic field and the magnetic dipole moment can be used to express Eq. (3.2) as below:

$$F = \begin{bmatrix} m_x & m_y & m_z & 0 & 0 \\ 0 & m_x & 0 & m_y & m_z \\ -m_z & 0 & m_x & -m_z & m_y \end{bmatrix} \begin{bmatrix} \frac{\partial B_x}{\partial x} \\ \frac{\partial B_x}{\partial y} \\ \frac{\partial B_x}{\partial z} \\ \frac{\partial B_y}{\partial y} \\ \frac{\partial B_y}{\partial z} \end{bmatrix} \qquad (3.5)$$

Equations (3.4) and (3.5) state that a rotating magnetic moment will be created when the magnetic dipole moment is not aligned with the direction of the external magnetic field. The

magnetic moment tries to align the magnetic dipole moment vector of the magnetic robot with the direction of the magnetic field. When the magnetic dipole moment and the magnetic field are aligned, the magnetic force will move the magnetic robot in the same direction as the magnetic field [76].

Kummer et al. [71] introduced the OctoMag system which was based on the idea of superimposing a magnetic field generated from soft magnetic core electromagnets. In a nutshell, the magnetic field at_point P can be calculated by summation of the magnetic field contribution of each electromagnet e. The magnitude of the vector $\tilde{B}_e(P)$ varies linearly with the electromagnet current and may be defined as a unit-current vector in units T/A. By multiplying by a scalar current value in units A, it can be used to represent the magnetic field produced by this electromagnet.

$$B_e(P) = \tilde{B}_e(P) i_e \qquad (3.6)$$

When using soft-magnetic cores, the field generated depends on both the current flowing through each electromagnet's core and the current flowing through the cores of all the other electromagnets in the system. We can assume that the field contributions of the individual currents superimpose linearly if the core material approaches an ideal soft-magnetic material, and the cores are kept inside their linear magnetization zones. The unit-field contribution matrix B(P) can be used to represent this in matrix form:

$$B(P) = [\tilde{B}_1(P) \quad \dots \quad \tilde{B}_n(P)] \begin{bmatrix} i_1 \\ \vdots \\ i_n \end{bmatrix} = \mathcal{B}(P) I \, (3.7)$$

Applying the same concept, the contributions from each of the currents can be used to express the gradient of the field in a particular frame, such as the x direction:

$$\frac{\partial B(P)}{\partial x} = \begin{bmatrix} \frac{\partial \tilde{B}_1(P)}{\partial x} & \dots & \frac{\partial \tilde{B}_n(P)}{\partial x} \end{bmatrix} \begin{bmatrix} i_1 \\ \vdots \\ i_n \end{bmatrix} = \mathcal{B}_x(P) I \quad (3.8)$$

These equations can be rearranged as follows if we are only concerned with creating a magnetic field and a magnetic field gradient:

$$\begin{bmatrix} B \\ \nabla \end{bmatrix} = \begin{bmatrix} \mathcal{B}(P) \\ \hat{B}^T \mathcal{B}_x(P) \\ \hat{B}^T \mathcal{B}_y(P) \\ \hat{B}^T \mathcal{B}_z(P) \end{bmatrix} \begin{bmatrix} i_1 \\ \vdots \\ i_n \end{bmatrix} = \mathcal{A}(\hat{B}, P) I \quad (3.9)$$

Where $\hat{B}$ represents B's unit vector. Using a 6-n actuation matrix $\mathcal{A}(\hat{B}, P)$, that dependents on the magnetic field's orientation and the set point, electromagnets currents are calculated from the magnetic field and gradient. The pseudoinverse can be used to determine the currents for a desired magnetic field and magnetic gradient vector that best solve for the target:

$$I = \mathcal{A}(\hat{B}, P)^* \begin{bmatrix} B \\ \nabla \end{bmatrix} \quad (3.10)$$

Using eq. (3.4) and (3.5), this derivation can be used to control the magnet’s torque and/or force.

Chapter 4 Experimental Methods:

The work in this thesis is divided into two main parts: the design and manufacturing of the magnetic actuation system, and the design and fabrication of the capsule endoscope.

4.1 Design and Manufacturing of the Actuation System:

4.1.1 System implementation:

An electromagnetic system is designed to generate a magnetic field to control the capsule precisely. The system is composed of 8 electromagnetic coils with a metallic core. The configuration of the actuation system is illustrated in Figure 4.1b. The coil base and the frame that holds the coils are made of aluminium. Each coil is made of 530 turns of copper wire (Ø1.2mm) wrapped over a steel core (Ø30 mm, L 90 mm). The final dimensions of each coil are Ø = 52 mm, and L = 90 mm, as shown in Figure 4.1a. Each coil is derived by DC motor driver BTS7960B and controlled by the PWM channel of Raspberry Pi 3 model B. The system is powered by two DC power supplies (24 V, 20 A).

The control algorithm is coded in Python 3 and run by the Raspberry Pi 3 Model B. The control algorithm is based on equation 3.10 described in the previous chapter. The set point can be set at the origin of the working space (0,0) to achieve open-loop control; however, we used image processing position feedback to close the loop to control the magnetic field at the captured position of the magnet. The position feedback was provided by a webcam connected to the USB port of the Raspberry Pi, as shown in Figure 4.1C.

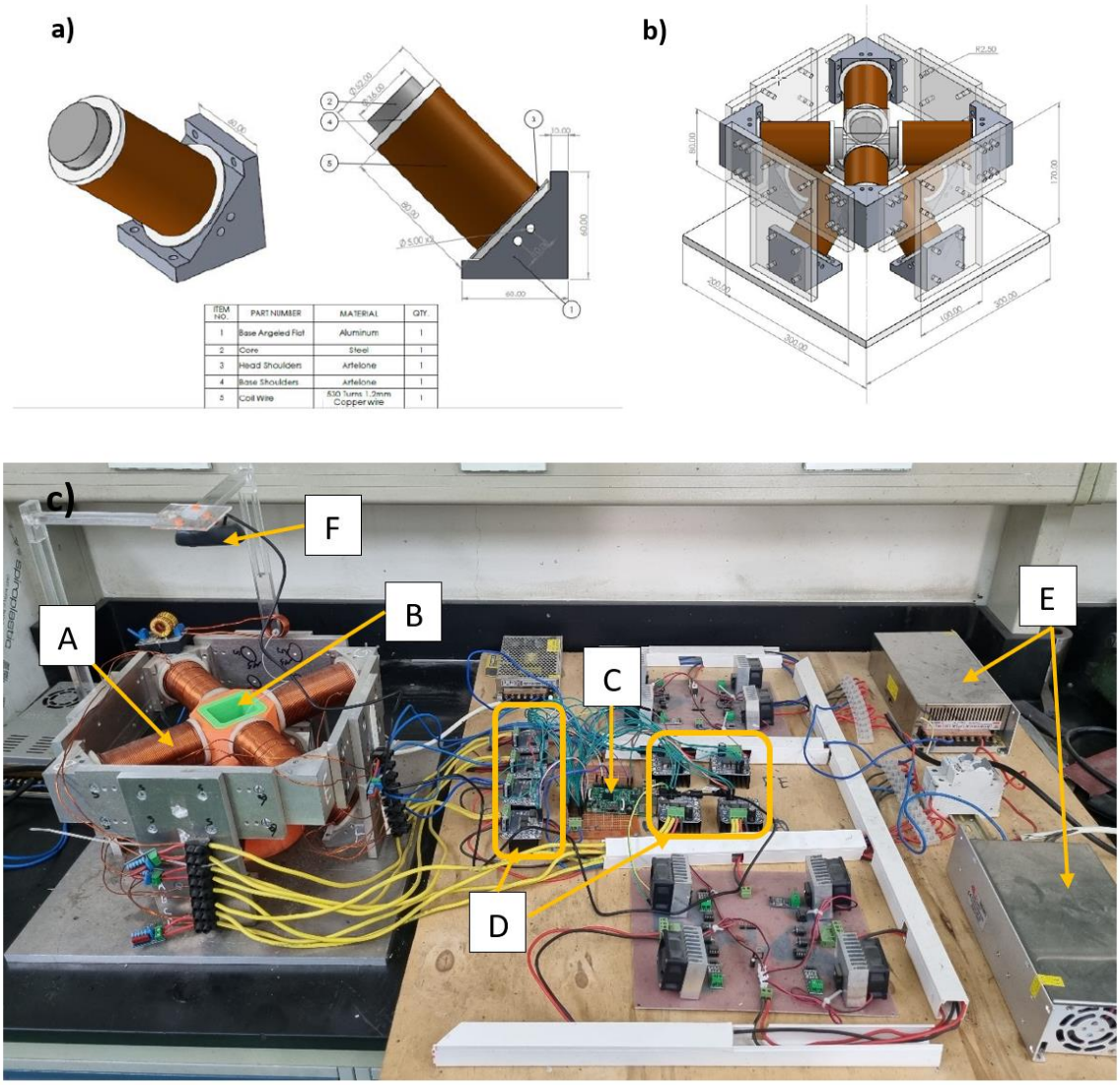

Figure 4-1: Overview of the electromagnetic system: (a) Electromagnetic coil design and its aluminium base. (b) CAD model of the actuation system. c) Photographs of the actual electromagnetic actuation setup. (c) Overview; A: 8 electromagnetic coils; B: Working space 40 x 40 x 40 mm for the capsule; C: Raspberry Pi 3 Model B that controls the whole system; D: 8 DC motor drivers BTS7960B; E: two DC power supplies (24 V, 20 A). F: Webcam for position feedback.

4.1.2 Field-Current Mapping:

The magnetic field of the final system is measured to generate the unit-current field map of each electromagnetic coil. The mapping process is done by measuring 3D magnetic field measurements when feeding one coil at a time with unit current (1 A). These measurements are taken at 125 points in the workspace arranged in a cubic 5 x 5 x 5 grid pattern and the distance between each point is 5 mm. Then, in real-time control, these data are interpolated. The mapping process is a very critical step of the study because the measurement errors will have a significant effect on the precision of the controller; hence, we used an Alpha Lab Inc. Vector/Magnitude 3D Gauss Meter Model VGM to measure the x, y, and z components of the magnetic field.

4.2 Design and Fabrication of the Capsule Endoscope:

The capsule is designed to deliver the chemical drug to a specific location. The capsule consists of two main parts, SMA actuated micropump and a pilot robot. The two parts are connected through a fine tube (Ø0.5 mm), as shown in Figure 4.3(a).

The micropump is based on the shape memory alloy micropump represented by Kotb. et al [77]. The concept behind the micropump is wrapping SMA wires around a flexible material. When the SMA is heated, it transforms the heat energy into a linear displacement, which causes the drug to be infused through a one-way valve into the targeted location. In the previous study [77], the SMA was heated by applying current to it; however, applying current to the capsule while being inside the GI tract requires the capsule to be threaded which causes discomfort to the patient. In order to actuate the capsule wirelessly, we heated the SMA using AC induction heating. NiTi SMA wires (Ø 0.4 mm) were acquired from Kellogg's Research Lab, USA. The SMA wires have a transition temperature of 45 C. We glued iron flakes to the NiTi wires to be heated wirelessly by AC induction. The micropump enclosure material is

Ecoflex 00-30 platinum silicone (Table 4.1). It was chosen because it is a flexible polymer with enough stiffness to follow the SMA shape. Moreover, Ecoflex 00-30 platinum silicone can be cured at a temperature lower than the transition temperature of the NiTi SMA wire. The SMA micropump manufacturing process was reported by Kotb et al.[77]. The inner pump structure was created by curing the Ecoflex in a 3D-printed mold. The SMA wire with iron flakes was then wrapped three times along the helical loops of the inner structure, as shown in Fig 4.2c. Next, the inner structure is put together with the outer capsule using a 3D-printed mold. Ecoflex 00-30 is used to shape the drug chamber in an aluminium mold. After that, the inner and outer one-return valves are fabricated using a stereolithography printer and are made of flexible 80 A resin by Formlabs, USA. A casing was used to hold the inner valve and the drug chamber. Additionally, it supports one end of the pump so that when the SMA spring contracts, the volume of the pump is pushed out without constricting the chamber. Figure 4.2a-e illustrates the steps of the pump fabrication, retrieved from [77].

Table 4.1: Ecoflex 00-30 material properties (retrieved from [78])

Material property	**Value**
Mixed Viscosity [Pa.s]	3
Specific Gravity [g/cm3]	1.07
Shore Hardness [ASTM D-2240]	00-30
Tear Strength [N/mm]	6.65
Tensile Strength [MPa]	1.38
Elongation at break [%]	900
Shrinkage [mm/mm]	<0.001
Curing Time at Room Temperature [h]	4

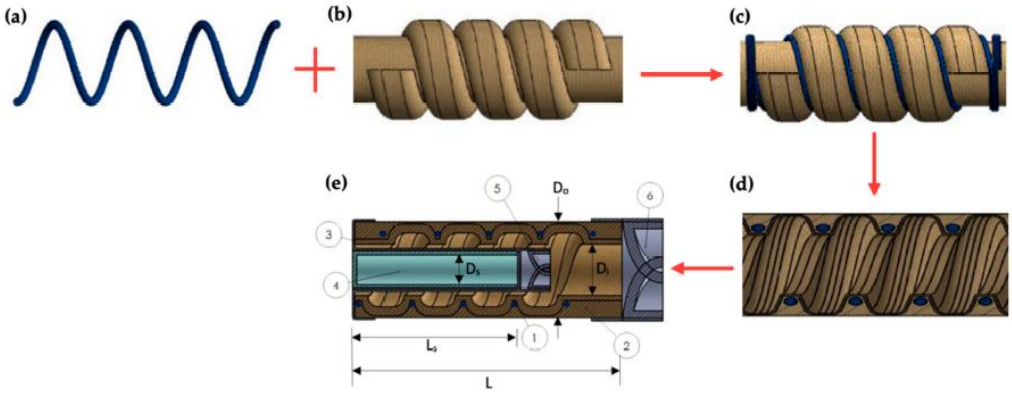

Figure 4-2: SMA micropump manufacturing process (a-e) manufacturing process flow, (e) show a schematic of the assembled pump: 1: SMA wire with iron flakes, 2: Silicon rubber, 3: casing, 4: drug chamber, 5: inner valve, and 6: outer valve – retrieved from [77].

The second part of the capsule is the pilot robot, and it consists of a chamber with microneedles and a cap that holds an NdFeB N52 (Ø 6 mm) magnet to be magnetically controlled by the electromagnetic actuation system described in section 4.1. The chamber and the cap are 3D-printed through a stereolithography printer and are made of ABS (Acrylonitrile Butadiene Styrene). The actual fabricated capsule is shown in Figure 4.3a.

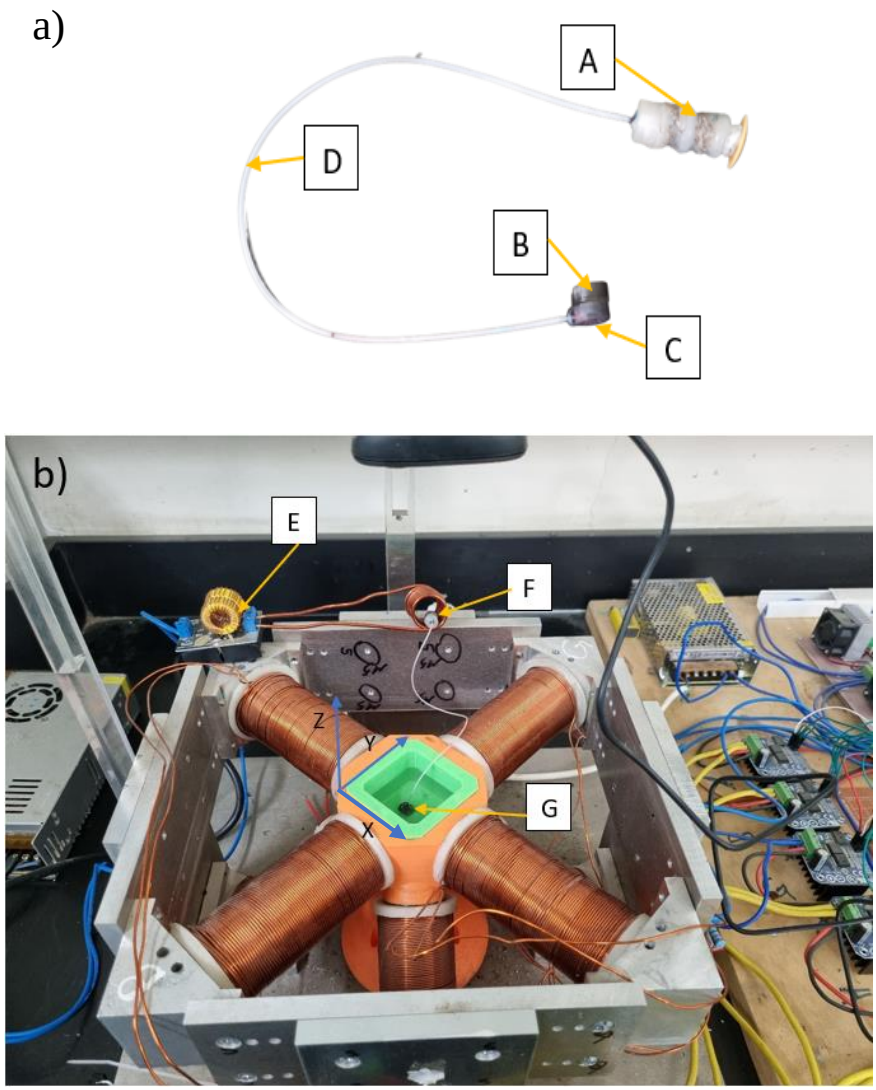

Figure 4-3: Overview of the capsule and its actuation system (a) Prototype of the capsule. A: The SMA-actuated micropump; B: the cap of the pilot robot and an NdFeB N52 (Ø 6 mm) magnet; C: The chamber of the pilot robot with microneedles on the bottom. D: Tube (Ø 0.5 mm) that connects the micropump with the pilot robot. (b) close-up view of the working space; E: the induction heating system 120W that is used to actuate the micropump of the capsule; F: Part 1 of the capsule, the micropump; G: Part 2 of the capsule, the pilot robot (Ø 6 mm, L 6 mm)

Chapter 5 Results and Discussions

In this chapter, the results of the experiments are illustrated.

5.1 Field-Current Mapping Result:

As described before, the unit current magnetic field maps are generated for each electromagnetic coil. Fig. 5.1 shows the unit current field maps of one of the coils.

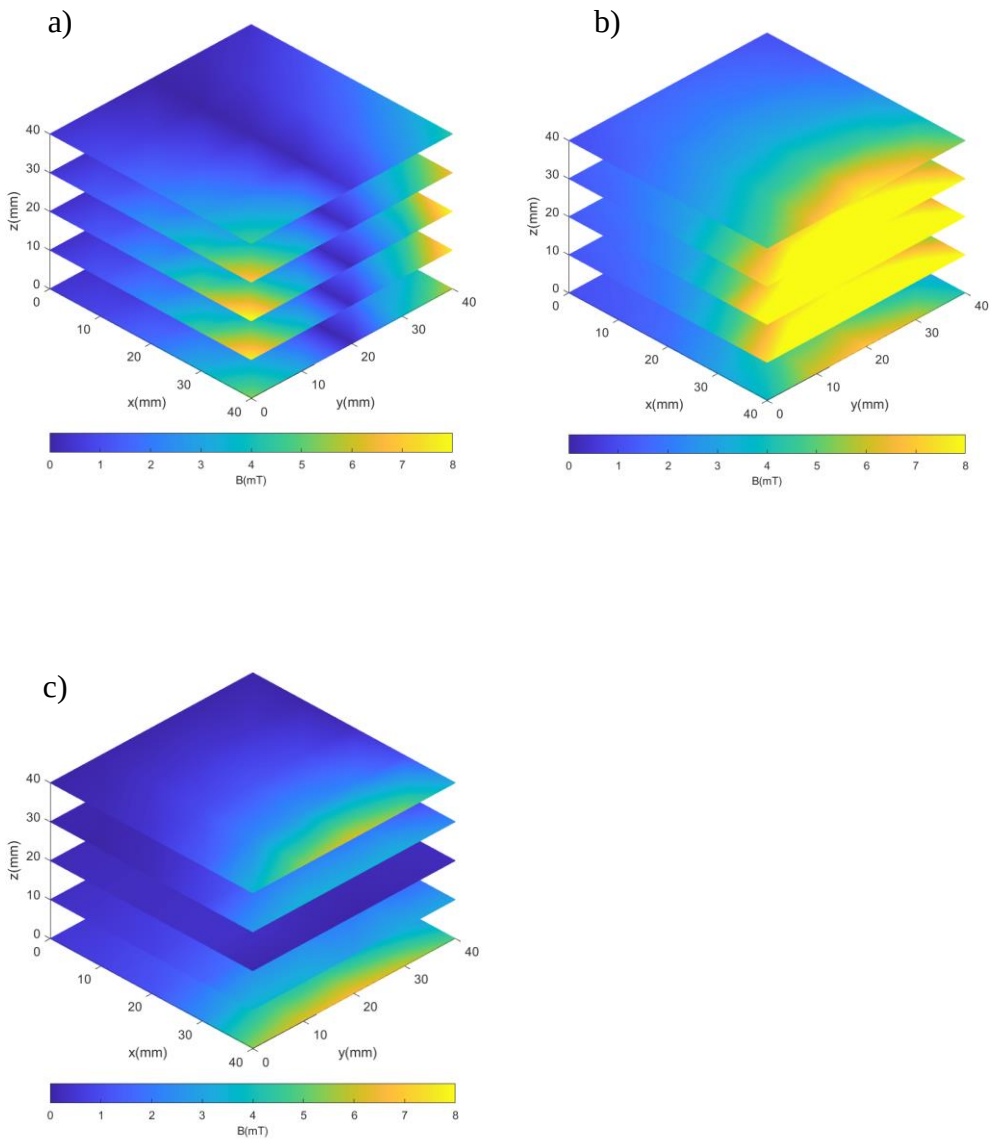

Figure 5-1: Unit current magnetic field maps (a) map for x component of the magnetic field B_x, (b) map for y component of the magnetic field B_y, (c) map for z component of the magnetic field B_z

From the measured magnetic field unit-current maps, we can interpolate the magnetic field at any point $\mathcal{B}(P)$ and calculate its gradient $\mathcal{B}_x(P)$, $\mathcal{B}_y(P)$, $\mathcal{B}_z(P)$ to be used in the control algorithm.

5.2 Control Algorithm of the Capsule:

The control starts by showing the operator a real-time image of the workspace; then the operator enters the desired path as shown in Fig 5.2.

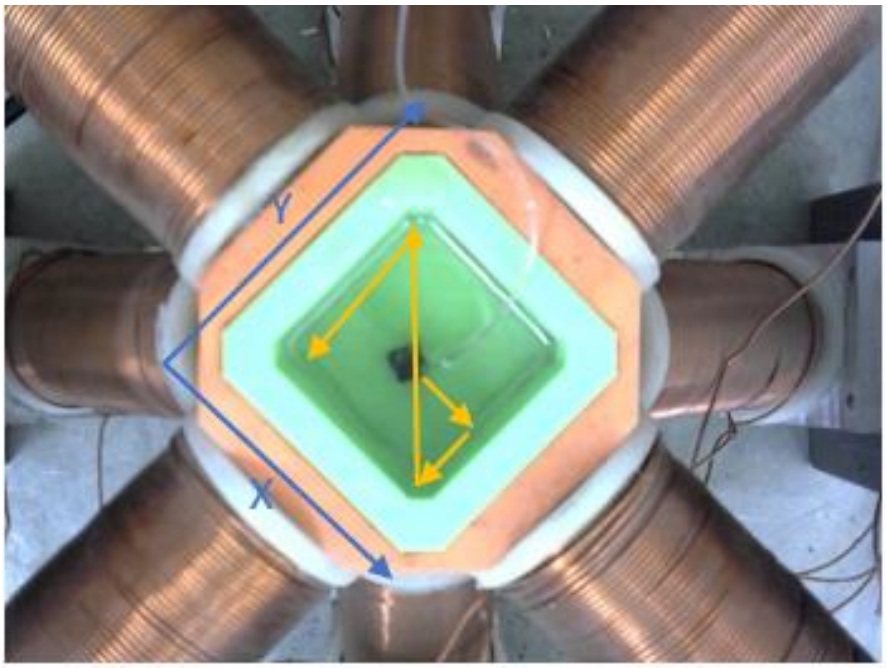

Figure 5-2: Example of the real-time image that appears to the operator to enter the desired path. The yellow line in the figure indicates the entered path.

The control algorithm calculates the required current for each electromagnetic coil to achieve the required motion. The algorithm uses the magnetic field unit-current maps that have been generated before in the previous section to interpolate the magnetic field at any point $\mathcal{B}(P)$ and calculate its gradient $\mathcal{B}_x(P)$, $\mathcal{B}_y(P)$, $\mathcal{B}_z(P)$. Using Eq. 3.10, we can calculate the required current for each electromagnetic coil to generate a specific magnetic field B and gradient ∇ at point *P*.

To linearize the controller, we choose a constant value for the magnetic field. Here we set |B| = 15 mT. The magnetic gradient is set to the desired steering vector. For simplified control, the point *P* can be set at the origin, However, this control method limits the effective workspace of the capsule. Hence, an enhanced control algorithm has been applied, using image processing feedback to calculate the real-time position of the capsule *P*. The code that runs the control algorithm is shown in Appendix A.

Fig 5.3 shows the motion of the capsule. When the pilot robot reaches the final position, the operator can press a button to actuate the induction heating system to heat the SMA in the micropump. It releases the drug through the microneedles on the pilot robot. It takes almost 52 sec to actuate the micropump using induction.

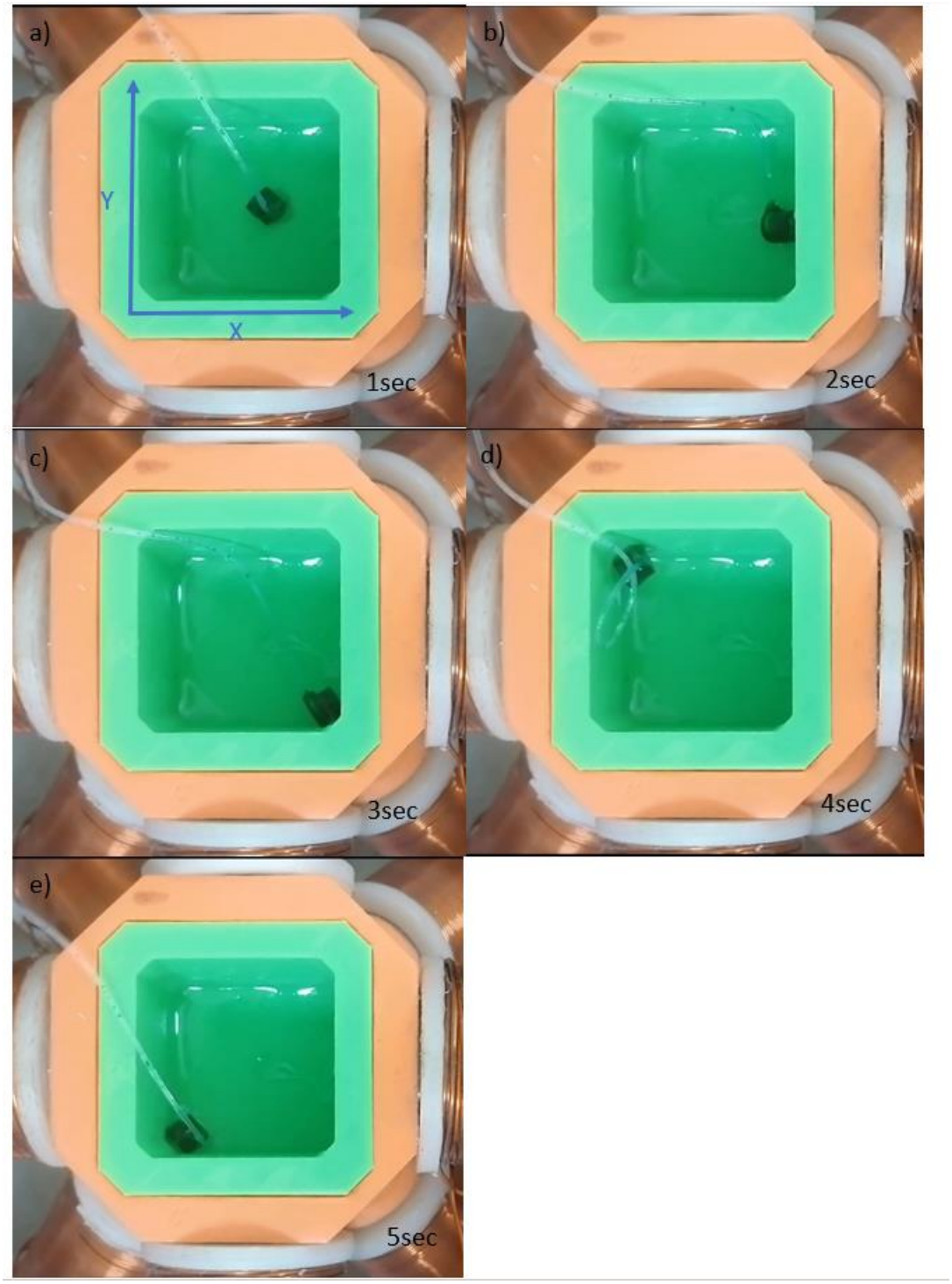

Figure 5-3: Results of enhanced control of the capsule. The images (a-e) show snapshots of the pilot robot that follows the entered path.

5.3 Discussion:

We introduced the design of a magnetically actuated capsule endoscope to improve the accuracy of the GI tract diagnosis and the ability to deliver drugs to specific locations. The unstructured and complex GI tract environments place high demands on the control accuracy of the electromagnetic systems. To enhance the controllability of the electromagnetic system, we generated the unit-current field maps by measuring the magnetic field explicitly instead of using FEM models as described in previous studies [59], [60], [69]. Moreover, an enhanced control algorithm has been developed and applied to increase the accuracy of the control and it can be used to maximize the workspace in future studies. Figure 5-4 shows the velocity and acceleration of the pilot robot in the first path, Figure 5-3a, b. The acceleration reaches 2000 mm/s^2 and the magnetic force reaches 1.3 mN, which is considered high for inner organs to sustain. However, in a larger workspace, the control can be optimized to control the velocity and acceleration of the capsule to be safer. The electromagnetic system has been able to steer the capsule endoscope successfully in the x-y plane, as shown in Figure 5-3; moreover, the control algorithm can be used for 3-D control. Additionally, the proposed electromagnetic system can be used to actuate other untethered devices for drug delivery application such as helical microrobots [79]–[81], soft microrobots [82]–[84], MagnetoSperm [85], [86], IRONSperm [87], [88], spermbots [89], [90], and paramagnetic microparticles [91].

Furthermore, the capsule endoscope design plays a significant role in the diagnostic accuracy and the safety of the operation. Hence, we introduced a novel design for an untethered capsule endoscope. The capsule endoscope has a micro pump that can be actuated wirelessly through AC induction. This allows the capsule endoscope to be untethered which eases the discomfort of the operation and increases the safety. As a proof of concept, we actuate the micropump in the capsule by a small 120W AC heating system, which takes around 52 sec to actuate the micropump and deliver the drug to the required position.

a)

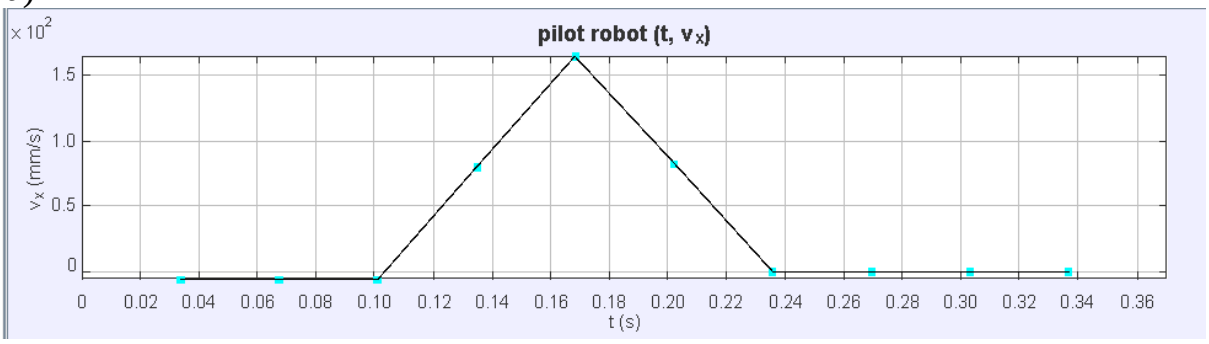

b)

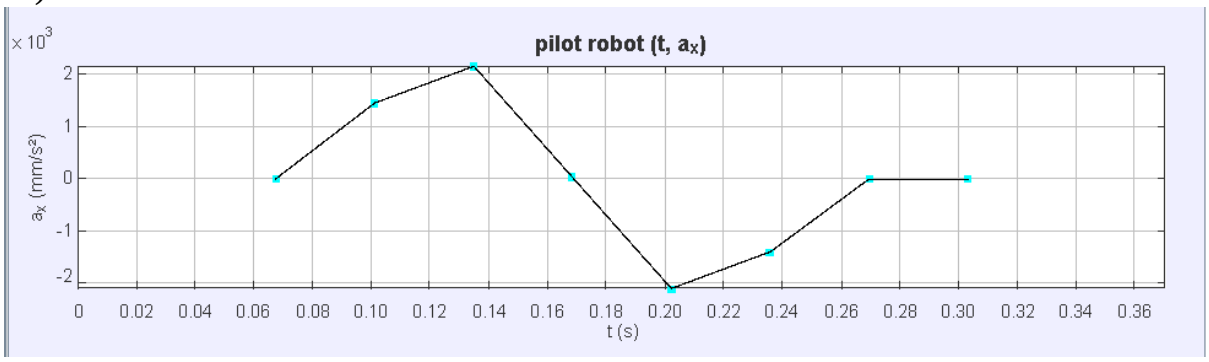

Figure 5-4 The measured velocity and acceleration of the pilot robot, a) The velocity in the y direction vs. time, b) The acceleration in the y direction vs. time.

Chapter 6 Conclusions and Future Work

Wireless capsule endoscopes (WCEs) have the potential to revolutionize present medical practice and greatly enhance the diagnostics and therapeutic procedures of GI tract cancers/diseases. Based on the literature review, the most promising method for wirelessly manipulating capsule endoscopes is magnetic actuation. Additionally, the current WCE systems are unable to control the motion of the WCE inside the GI tract and deliver drugs wirelessly. Therefore, the main aim of this thesis was to develop an electromagnetic system to wirelessly control capsule endoscopes and release drugs to a given location inside the GI tract.

The system consists of 8 stationary electromagnetic coils that generate a magnetic field to control the capsule. After manufacturing the prototype, unit-current field maps were generated for each coil to be used in the control algorithm. The control method is enhanced by integrating locomotion feedback using image processing, which improves the controllability of the capsule and allows for maximizing the effective working space. The prototype system can maneuver the capsule effectively in two directions; however, the system can provide 5-DOF control. Moreover, a novel capsule endoscope design has been introduced. We integrated a micro pump that can be actuated wirelessly by AC induction heating, to deliver drugs to an exact location inside the GI tract. The system is expected to have great capabilities in minimally invasive diagnosis and treatment for gastrointestinal (GI) tract cancer/diseases.

6.1 Future Works:

Although the proposed electromagnetic system provides promising results, further studies are necessary. One of the main areas to enhance is a closed-loop control algorithm to control the capsule's position inside the GI tract. Additionally, image processing locomotion feedback must be replaced by another method that can effectively capture the position of the

capsule inside the patient, for example, magnetic sensor arrays, or deep learning algorithms that can calculate the position of the capsule from the images captured by the capsule itself.

Appendix A: Python Code for Control and Image Processing

The code follows the control algorithm applied. It uses the previously measured unit-current field maps and then calculates interpolation operators to be used in real-time. After that, calculate the magnetic gradient.

```python

# function that show image to operator to select path
SPath = Mycv.GetPath()

print(SPath)
Nowr = Mycv.TakePic()
rdes = tuple(SPath[0])
r = tuple(np.subtract(rdes,Nowr))
print("r", r)
ndes = np.divide(r,np.linalg.norm(r))
Bo = np.multiply(ndes,0.015)

# Read unit-current maps for each coil then calculate interpolation opertaors and gradient
DataExcel = pd.ExcelFile('TestCali_PythonPos.xlsx')
for i in range(4):
    sheet = DataExcel.parse(i).to_numpy()

    data = sheet[0,:25].reshape(5,5)
    result = [val/10000 for val in data]

    interp = RegularGridInterpolator((points, points), result)
    InterpolatedBx.append(interp)
    Gradient = np.gradient(result, 0.01,axis = 0)

    Gradientxx.append(Gradient)
    Gradient = np.gradient(result, 0.01,axis = 1)
    Gradientxy.append(Gradient)

    data = sheet[1,:25].reshape(5,5)
    result = [val/10000 for val in data]
    interp = RegularGridInterpolator((points, points), result)
    InterpolatedBy.append(interp)
    Gradient = np.gradient(result, 0.01,axis = 0)
    Gradientyx.append(Gradient)
    Gradient = np.gradient(result, 0.01,axis = 1)
    Gradientyy.append(Gradient)


InterpolatedBx = np.array(InterpolatedBx)
InterpolatedBy = np.array(InterpolatedBy)
Gradientxx = np.array(Gradientxx)
Gradientxy = np.array(Gradientxy)
Gradientyx = np.array(Gradientyx)
Gradientyy = np.array(Gradientyy)

```

```python
#intialize Rasperry Pi PWM channels
Fn.StartGPIO()

# Calculate the required currents
for i in range(len(SPath)):
    rdes = tuple(SPath[i])
    r = tuple(np.subtract(rdes,Nowr))
    ndes = np.divide(r,np.linalg.norm(r))
    print("i", i, "r", r, "rdes", rdes, "ndes", ndes)
    Bo = np.multiply(ndes,0.015)
    B , Gx, Gy = Fn.mangeticMapping(rdes,InterpolatedBx,InterpolatedBy,Gradientxx,Gradientxy,Gradientyx,Gradientyy)
    Bdes = np.divide(B,np.linalg.norm(B))

    A = np.vstack((np.transpose(B),ndes@np.transpose(Gx),ndes@np.transpose(Gy)))

    D = np.transpose(np.hstack((Bo,ndes)))

    Iout = np.linalg.pinv(A)@D


    Fn.WriteCurrent(Iout)
    while True:
        print(tuple(Mycv.TakePic()))
        if rdes == tuple(Mycv.TakePic()):
            break

    Nowr = rdes

input("close")
Fn.StopCoils()
time.sleep(0.1)
Fn.cleanPins()
print("Coils stops")
```

Below is the code that runs the image processing code that returns the position of the capsule:

```
def GetPath():
      ## Funcrion that show image to operator and ask to enter the path required.

      check, img = webcam.read()
      grayI = cv2.cvtColor(img, cv2.COLOR_BGR2GRAY)
      img180 = cv2.rotate(grayI, cv2.ROTATE_180)
      rotatedI = ndimage.rotate(img180, -45)

      cropI = rotatedI[635:945, 590:900]
      cv2.namedWindow('Point Coordinates')
      cv2.setMouseCallback('Point Coordinates', click_event)

      while True:
            cv2.imshow('Point Coordinates',cropI)
            k = cv2.waitKey(1) & 0xFF
            if k == 27:
                  break
      return Path
def click_event(event, x, y, flags, params):
   if event == cv2.EVENT_LBUTTONDOWN:
      print(f'({x},{y})')

      # put coordinates as text on the image
      cv2.putText(img, f'({x},{y})',(x,y),
      cv2.FONT_HERSHEY_SIMPLEX, 1, (0, 0, 255), 2)

      # draw point on the image
      cv2.circle(img, (x,y), 3, (0,255,255), -1)
      Path.append([round((y* pixel2cm),2) ,round((x* pixel2cm),2)])

def TakePic():
      ## Function to get the current position from the image.
      check, img = webcam.read()
      grayI = cv2.cvtColor(img, cv2.COLOR_BGR2GRAY)
      img180 = cv2.rotate(grayI, cv2.ROTATE_180)
      rotatedI = ndimage.rotate(img180, -45)

      cropI = rotatedI[635:945, 590:900]
      ret,img_bin = cv2.threshold(cropI, 100, 255, cv2.THRESH_BINARY) # imbinarize(cropI,0.25)
      cv2.imshow('Bin',img_bin)
      n_labels, labels, stats, centroids = cv2.connectedComponentsWithStats(img_bin,connectivity=4)
      P = (round((centroids[0,1] * pixel2cm),2), round((centroids[0,0] * pixel2cm),2))
      return P
```

References:

[1] R. L. Siegel, K. D. Miller, H. E. Fuchs, and A. Jemal, "Cancer statistics, 2022," *CA. Cancer J. Clin.*, vol. 72, no. 1, pp. 7–33, 2022, doi: 10.3322/caac.21708.

[2] R. K. Jain and T. Stylianopoulos, "Delivering nanomedicine to solid tumors," *Nat. Rev. Clin. Oncol.*, vol. 7, no. 11, pp. 653–664, Nov. 2010, doi: 10.1038/nrclinonc.2010.139.

[3] I. F. Tannock, C. M. Lee, J. K. Tunggal, D. S. M. Cowan, and M. J. Egorin, "Limited Penetration of Anticancer Drugs through Tumor Tissue: A Potential Cause of Resistance of Solid Tumors to Chemotherapy," *Clin. Cancer Res.*, vol. 8, no. 3, pp. 878–884, Mar. 2002.

[4] R. Grantab, S. Sivananthan, and I. F. Tannock, "The Penetration of Anticancer Drugs through Tumor Tissue as a Function of Cellular Adhesion and Packing Density of Tumor Cells," *Cancer Res.*, vol. 66, no. 2, pp. 1033–1039, Jan. 2006, doi: 10.1158/0008-5472.CAN-05-3077.

[5] G. Berci and K. A. Forde, "History of endoscopy: what lessons have we learned from the past?," *Surg. Endosc.*, vol. 14, no. 1, pp. 5–15, Jan. 2000, doi: 10.1007/s004649900002.

[6] G. Iddan, G. Meron, A. Glukhovsky, and P. Swain, "Wireless capsule endoscopy," *Nature*, vol. 405, no. 6785, Art. no. 6785, May 2000, doi: 10.1038/35013140.

[7] "Global Health Observatory (GHO) Data, Cancer Survival." https://gco.iarc.fr/survival/survmark/ (accessed Sep. 04, 2023).

[8] D. Ramai, K. Zakhia, D. Etienne, and M. Reddy, "Philipp Bozzini (1773-1809): The earliest description of endoscopy," *J. Med. Biogr.*, vol. 26, no. 2, pp. 137–141, May 2018, doi: 10.1177/0967772018755587.

[9] H. Mateen, R. Basar, A. U. Ahmed, and M. Y. Ahmad, "Localization of Wireless Capsule Endoscope: A Systematic Review," *IEEE Sens. J.*, vol. 17, no. 5, pp. 1197–1206, Mar. 2017, doi: 10.1109/JSEN.2016.2645945.

[10] M. R. Basar, F. Malek, K. M. Juni, M. S. Idris, and M. I. M. Saleh, "Ingestible Wireless Capsule Technology: A Review of Development and Future Indication," *Int. J. Antennas Propag.*, vol. 2012, pp. 1–14, 2012, doi: 10.1155/2012/807165.

[11] C. P. Swain, F. Gong, and T. N. Mills, "Wireless transmission of a colour television moving image from the stomach using a miniature CCD camera, light source and microwave transmitter," *Gastrointest. Endosc.*, vol. 4, no. 45, p. AB40, 1997, doi: 10.1016/S0016-5107(97)80063-6.

[12] A. Moglia, A. Menciassi, M. O. Schurr, and P. Dario, "Wireless capsule endoscopy: from diagnostic devices to multipurpose robotic systems," *Biomed. Microdevices*, vol. 9, no. 2, pp. 235–243, Apr. 2007, doi: 10.1007/s10544-006-9025-3.

[13] H. Dehghani *et al.*, "Design and preliminary evaluation of a self-steering, pneumatically driven colonoscopy robot," *J. Med. Eng. Technol.*, vol. 41, no. 3, pp. 223–236, Apr. 2017, doi: 10.1080/03091902.2016.1275853.

[14] H. Heung, P. W. Y. Chiu, and Z. Li, "Design and prototyping of a soft earthworm-like robot targeted for GI tract inspection," in *2016 IEEE International Conference on Robotics and Biomimetics (ROBIO)*, Dec. 2016, pp. 497–502. doi: 10.1109/ROBIO.2016.7866371.

[15] Y. Li, H. Liu, S. Hao, H. Li, J. Han, and Y. Yang, "Design and control of a novel gastroscope intervention mechanism with circumferentially pneumatic-driven clamping function," *Int. J. Med. Robot.*, vol. 13, no. 1, p. e1745, 2017, doi: 10.1002/rcs.1745.

[16] D. Lee, S. Joe, J. Choi, B.-I. Lee, and B. Kim, "An elastic caterpillar-based self-propelled robotic colonoscope with high safety and mobility," *Mechatronics*, vol. 39, pp. 54–62, Nov. 2016, doi: 10.1016/j.mechatronics.2016.08.002.

[17] K. Wang, J. Ma, F. Wang, Z. Wang, G. Yan, and Y. Zhou, “Full-driving soft robotic colonoscope in compliant colon tissue,” *J. Med. Eng. Technol.*, vol. 41, no. 8, pp. 662–669, Nov. 2017, doi: 10.1080/03091902.2017.1394387.
[18] P. Valdastri, R. J. Webster, C. Quaglia, M. Quirini, A. Menciassi, and P. Dario, “A New Mechanism for Mesoscale Legged Locomotion in Compliant Tubular Environments,” *IEEE Trans. Robot.*, vol. 25, no. 5, pp. 1047–1057, Oct. 2009, doi: 10.1109/TRO.2009.2014127.
[19] J. Liu, L. Yin, J. H. Chandler, X. Chen, P. Valdastri, and S. Zuo, “A dual-bending endoscope with shape-lockable hydraulic actuation and water-jet propulsion for gastrointestinal tract screening,” *Int. J. Med. Robot.*, vol. 17, no. 1, p. e2197, 2021, doi: 10.1002/rcs.2197.
[20] M. Kang, S. Joe, T. An, H. Jang, and B. Kim, “A novel robotic colonoscopy system integrating feeding and steering mechanisms with self-propelled paddling locomotion: A pilot study,” *Mechatronics*, vol. 73, p. 102478, Feb. 2021, doi: 10.1016/j.mechatronics.2020.102478.
[21] J. J. Abbott, E. Diller, and A. J. Petruska, “Magnetic Methods in Robotics,” *Annu. Rev. Control Robot. Auton. Syst.*, vol. 3, no. 1, pp. 57–90, 2020, doi: 10.1146/annurev-control-081219-082713.
[22] H.-J. Chung, A. M. Parsons, and L. Zheng, “Magnetically Controlled Soft Robotics Utilizing Elastomers and Gels in Actuation: A Review,” *Adv. Intell. Syst.*, vol. 3, no. 3, p. 2000186, 2021, doi: 10.1002/aisy.202000186.
[23] H. Tillander, “Magnetic Guidance of a Catheter with Articulated Steel Tip,” *Acta Radiol.*, vol. 35, no. 1, pp. 62–64, Jan. 1951, doi: 10.3109/00016925109136646.
[24] “Experimental study of the magnetic stereotaxis system for catheter manipulation within the brain in: Journal of Neurosurgery Volume 93 Issue 2 (2000) Journals.” https://thejns.org/view/journals/j-neurosurg/93/2/article-p282.xml (accessed Jul. 11, 2023).
[25] “OctoMag: An electromagnetic system for 5-DOF wireless micromanipulation - IEEE Conference Publication.” https://ieeexplore-ieee-org.libproxy.aucegypt.edu/document/5509857 (accessed Sep. 21, 2019).
[26] J. Sikorski, A. Denasi, G. Bucchi, S. Scheggi, and S. Misra, “Vision-Based 3-D Control of Magnetically Actuated Catheter Using BigMag—An Array of Mobile Electromagnetic Coils,” *IEEEASME Trans. Mechatron.*, vol. 24, no. 2, pp. 505–516, Apr. 2019, doi: 10.1109/TMECH.2019.2893166.
[27] “Dynamically Shaped Magnetic Fields | Circulation: Arrhythmia and Electrophysiology.” https://www.ahajournals.org/doi/full/10.1161/CIRCEP.110.959692 (accessed Jul. 11, 2023).
[28] K. T. Nguyen *et al.*, “A Magnetically Guided Self-Rolled Microrobot for Targeted Drug Delivery, Real-Time X-Ray Imaging, and Microrobot Retrieval,” *Adv. Healthc. Mater.*, vol. 10, no. 6, p. 2001681, 2021, doi: 10.1002/adhm.202001681.
[29] D. Jang, J. Jeong, H. Song, and S. K. Chung, “Targeted drug delivery technology using untethered microrobots: a review,” *J. Micromechanics Microengineering*, vol. 29, no. 5, p. 053002, Mar. 2019, doi: 10.1088/1361-6439/ab087d.
[30] W. Chen, J. Sui, and C. Wang, “Magnetically Actuated Capsule Robots: A Review,” *IEEE Access*, vol. 10, pp. 88398–88420, 2022, doi: 10.1109/ACCESS.2022.3197632.
[31] M. Szalai *et al.*, “First prospective European study for the feasibility and safety of magnetically controlled capsule endoscopy in gastric mucosal abnormalities,” *World J. Gastroenterol.*, vol. 28, no. 20, pp. 2227–2242, May 2022, doi: 10.3748/wjg.v28.i20.2227.

[32] F. Carpi, S. Galbiati, and A. Carpi, “Controlled Navigation of Endoscopic Capsules: Concept and Preliminary Experimental Investigations,” *IEEE Trans. Biomed. Eng.*, vol. 54, no. 11, pp. 2028–2036, Nov. 2007, doi: 10.1109/TBME.2007.894729.
[33] P. Valdastri *et al.*, “A magnetic internal mechanism for precise orientation of the camera in wireless endoluminal applications,” *Endoscopy*, vol. 42, no. 6, pp. 481–486, Jun. 2010, doi: 10.1055/s-0029-1244170.
[34] G. Pittiglio *et al.*, “Magnetic Levitation for Soft-Tethered Capsule Colonoscopy Actuated With a Single Permanent Magnet: A Dynamic Control Approach,” *IEEE Robot. Autom. Lett.*, vol. 4, pp. 1224–1231, Apr. 2019.
[35] L. Barducci, G. Pittiglio, J. C. Norton, K. L. Obstein, and P. Valdastri, “Adaptive Dynamic Control for Magnetically Actuated Medical Robots,” *IEEE Robot. Autom. Lett.*, vol. 4, no. 4, pp. 3633–3640, Oct. 2019, doi: 10.1109/LRA.2019.2928761.
[36] I. Rahman *et al.*, “Magnetic-assisted capsule endoscopy in the upper GI tract by using a novel navigation system (with video),” *Gastrointest. Endosc.*, vol. 83, no. 5, pp. 889-895.e1, May 2016, doi: 10.1016/j.gie.2015.09.015.
[37] Y.-C. Lin, C.-L. Chen, Y.-W. Kao, C.-Y. Chang, M.-C. Chen, and C.-K. Liu, “Feasibility of Upper Gastrointestinal Examination in Home Care Setting with a Magnetically Assisted Capsule Endoscopy System: A Retrospective Study,” *Healthcare*, vol. 9, no. 5, Art. no. 5, May 2021, doi: 10.3390/healthcare9050577.
[38] G. Ciuti *et al.*, “Robotic versus manual control in magnetic steering of an endoscopic capsule,” *Endoscopy*, pp. 148–152, Dec. 2009, doi: 10.1055/s-0029-1243808.
[39] G. Ciuti, P. Valdastri, A. Menciassi, and P. Dario, “Robotic magnetic steering and locomotion of capsule endoscope for diagnostic and surgical endoluminal procedures,” *Robotica*, vol. 28, pp. 199–207, 2010, doi: 10.1017/s0263574709990361.
[40] A. W. Mahoney and J. J. Abbott, “Managing magnetic force applied to a magnetic device by a rotating dipole field,” *Appl. Phys. Lett.*, vol. 99, no. 13, p. 134103, Sep. 2011, doi: 10.1063/1.3644021.
[41] A. W. Mahoney, D. L. Cowan, K. M. Miller, and J. J. Abbott, “Control of untethered magnetically actuated tools using a rotating permanent magnet in any position,” in *2012 IEEE International Conference on Robotics and Automation*, May 2012, pp. 3375–3380. doi: 10.1109/ICRA.2012.6225097.
[42] K. M. Miller, A. W. Mahoney, T. Schmid, and J. J. Abbott, “Proprioceptive magnetic-field sensing for closed-loop control of magnetic capsule endoscopes,” in *2012 IEEE/RSJ International Conference on Intelligent Robots and Systems*, Oct. 2012, pp. 1994–1999. doi: 10.1109/IROS.2012.6385708.
[43] A. W. Mahoney, S. E. Wright, and J. J. Abbott, “Managing the attractive magnetic force between an untethered magnetically actuated tool and a rotating permanent magnet,” in *2013 IEEE International Conference on Robotics and Automation*, May 2013, pp. 5366–5371. doi: 10.1109/ICRA.2013.6631346.
[44] A. W. Mahoney and J. J. Abbott, “Generating Rotating Magnetic Fields With a Single Permanent Magnet for Propulsion of Untethered Magnetic Devices in a Lumen,” *IEEE Trans. Robot.*, vol. 30, no. 2, pp. 411–420, Apr. 2014, doi: 10.1109/TRO.2013.2289019.
[45] A. Arezzo *et al.*, “Experimental assessment of a novel robotically-driven endoscopic capsule compared to traditional colonoscopy,” *Dig. Liver Dis.*, vol. 45, no. 8, pp. 657–662, Aug. 2013, doi: 10.1016/j.dld.2013.01.025.
[46] A. W. Mahoney and J. J. Abbott, “Five-degree-of-freedom manipulation of an untethered magnetic device in fluid using a single permanent magnet with application in stomach capsule endoscopy,” *Int. J. Robot. Res.*, vol. 35, no. 1–3, pp. 129–147, Jan. 2016, doi: 10.1177/0278364914558006.

[47] K. M. Popek, T. Hermans, and J. J. Abbott, “First demonstration of simultaneous localization and propulsion of a magnetic capsule in a lumen using a single rotating magnet,” in *2017 IEEE International Conference on Robotics and Automation (ICRA)*, May 2017, pp. 1154–1160. doi: 10.1109/ICRA.2017.7989138.
[48] S. E. Wright, A. W. Mahoney, K. M. Popek, and J. J. Abbott, “The Spherical-Actuator-Magnet Manipulator: A Permanent-Magnet Robotic End-Effector,” *IEEE Trans. Robot.*, vol. 33, no. 5, pp. 1013–1024, Oct. 2017, doi: 10.1109/TRO.2017.2694841.
[49] B. Chaluvadi, K. M. Stewart, A. J. Sperry, H. C. Fu, and J. J. Abbott, “Kinematic Model of a Magnetic-Microrobot Swarm in a Rotating Magnetic Dipole Field,” *IEEE Robot. Autom. Lett.*, vol. 5, no. 2, pp. 2419–2426, Apr. 2020, doi: 10.1109/LRA.2020.2972857.
[50] X. Jiang, J. Pan, Z.-S. Li, and Z. Liao, “Standardized examination procedure of magnetically controlled capsule endoscopy,” *VideoGIE*, vol. 4, no. 6, pp. 239–243, Jun. 2019, doi: 10.1016/j.vgie.2019.03.003.
[51] Z. Liao *et al.*, “Accuracy of Magnetically Controlled Capsule Endoscopy, Compared With Conventional Gastroscopy, in Detection of Gastric Diseases,” *Clin. Gastroenterol. Hepatol.*, vol. 14, no. 9, pp. 1266-1273.e1, Sep. 2016, doi: 10.1016/j.cgh.2016.05.013.
[52] H. Lai *et al.*, “Standing-type magnetically guided capsule endoscopy versus gastroscopy for gastric examination: multicenter blinded comparative trial,” *Dig. Endosc.*, vol. 32, no. 4, pp. 557–564, 2020, doi: 10.1111/den.13520.
[53] C. Cheng, T. Sun, and H. Zhang, “Human gastric magnet-controlled capsule endoscopy conducted in a standing position: the phase 1 study,” *BMC Gastroenterol.*, vol. 19, no. 1, p. 184, Nov. 2019, doi: 10.1186/s12876-019-1101-2.
[54] S.-Y. Yen *et al.*, “Automatic lumen detection and magnetic alignment control for magnetic-assisted capsule colonoscope system optimization,” *Sci. Rep.*, vol. 11, no. 1, Art. no. 1, Mar. 2021, doi: 10.1038/s41598-021-86101-9.
[55] P. Swain *et al.*, “Remote magnetic manipulation of a wireless capsule endoscope in the esophagus and stomach of humans (with videos),” *Gastrointest. Endosc.*, vol. 71, no. 7, pp. 1290–1293, Jun. 2010, doi: 10.1016/j.gie.2010.01.064.
[56] J. Keller *et al.*, “Inspection of the human stomach using remote-controlled capsule endoscopy: a feasibility study in healthy volunteers (with videos),” *Gastrointest. Endosc.*, vol. 73, no. 1, pp. 22–28, Jan. 2011, doi: 10.1016/j.gie.2010.08.053.
[57] J. Keller *et al.*, “Remote magnetic control of a wireless capsule endoscope in the esophagus is safe and feasible: results of a randomized, clinical trial in healthy volunteers,” *Gastrointest. Endosc.*, vol. 72, no. 5, pp. 941–946, Nov. 2010, doi: 10.1016/j.gie.2010.06.053.
[58] H. Sun, J. Liu, and Q. Wang, “Magnetic Actuation Systems and Magnetic Robots for Gastrointestinal Examination and Treatment,” *Chin. J. Electr. Eng.*, vol. 9, no. 1, pp. 3–28, Mar. 2023, doi: 10.23919/CJEE.2023.000009.
[59] M. P. Kummer, J. J. Abbott, B. E. Kratochvil, R. Borer, A. Sengul, and B. J. Nelson, “OctoMag: An Electromagnetic System for 5-DOF Wireless Micromanipulation,” *IEEE Trans. Robot.*, vol. 26, no. 6, pp. 1006–1017, Dec. 2010, doi: 10.1109/TRO.2010.2073030.
[60] B. E. Kratochvil *et al.*, “MiniMag: A Hemispherical Electromagnetic System for 5-DOF Wireless Micromanipulation,” in *Experimental Robotics: The 12th International Symposium on Experimental Robotics*, O. Khatib, V. Kumar, and G. Sukhatme, Eds., in Springer Tracts in Advanced Robotics. Berlin, Heidelberg: Springer, 2014, pp. 317–329. doi: 10.1007/978-3-642-28572-1_22.
[61] S. Jeon, G. Jang, H. Choi, and S. Park, “Magnetic Navigation System With Gradient and Uniform Saddle Coils for the Wireless Manipulation of Micro-Robots in Human Blood

Vessels," *IEEE Trans. Magn.*, vol. 46, no. 6, pp. 1943–1946, Jun. 2010, doi: 10.1109/TMAG.2010.2040144.

[62] G. B. Jang, S. Jeon, J. Nam, W. Lee, and G. Jang, "A Spiral Microrobot Performing Navigating Linear and Drilling Motions by Magnetic Gradient and Rotating Uniform Magnetic Field for Applications in Unclogging Blocked Human Blood Vessels," *IEEE Trans. Magn.*, vol. 51, no. 11, pp. 1–4, Nov. 2015, doi: 10.1109/TMAG.2015.2436913.

[63] M. C. Hoang *et al.*, "Independent Electromagnetic Field Control for Practical Approach to Actively Locomotive Wireless Capsule Endoscope," *IEEE Trans. Syst. Man Cybern. Syst.*, vol. 51, no. 5, pp. 3040–3052, May 2021, doi: 10.1109/TSMC.2019.2917298.

[64] H. Keller *et al.*, "Method for navigation and control of a magnetically guided capsule endoscope in the human stomach," in *2012 4th IEEE RAS EMBS International Conference on Biomedical Robotics and Biomechatronics (BioRob)*, Jun. 2012, pp. 859–865. doi: 10.1109/BioRob.2012.6290795.

[65] J.-F. Rey *et al.*, "Blinded nonrandomized comparative study of gastric examination with a magnetically guided capsule endoscope and standard videoendoscope," *Gastrointest. Endosc.*, vol. 75, no. 2, pp. 373–381, Feb. 2012, doi: 10.1016/j.gie.2011.09.030.

[66] J. Liu *et al.*, "Design and Fabrication of a Catheter Magnetic Navigation System for Cardiac Arrhythmias," *IEEE Trans. Appl. Supercond.*, vol. 26, no. 4, pp. 1–4, Jun. 2016, doi: 10.1109/TASC.2016.2514265.

[67] D. Son, H. Gilbert, and M. Sitti, "Magnetically Actuated Soft Capsule Endoscope for Fine-Needle Biopsy," *Soft Robot.*, Sep. 2019, doi: 10.1089/soro.2018.0171.

[68] D. Son, S. Yim, and M. Sitti, "A 5-D Localization Method for a Magnetically Manipulated Untethered Robot Using a 2-D Array of Hall-Effect Sensors," *IEEEASME Trans. Mechatron.*, vol. 21, no. 2, pp. 708–716, Apr. 2016, doi: 10.1109/TMECH.2015.2488361.

[69] H. Sun, J. Liu, L. Wang, C. Niu, and Q. Wang, "A Novel Control Method of Magnetic Navigation Capsule Endoscope for Gastrointestinal Examination," *IEEE Trans. Magn.*, vol. 58, no. 1, pp. 1–9, Jan. 2022, doi: 10.1109/TMAG.2021.3124012.

[70] H. Sun *et al.*, "In vivo animal study of the magnetic navigation system for capsule endoscope manipulation within the esophagus, stomach, and colorectum," *Med. Phys.*, vol. 49, no. 11, pp. 6813–6823, 2022, doi: 10.1002/mp.15976.

[71] A. Koulaouzidis, D. K. Iakovidis, A. Karargyris, and E. Rondonotti, "Wireless endoscopy in 2020: Will it still be a capsule?," *World J. Gastroenterol. WJG*, vol. 21, no. 17, pp. 5119–5130, May 2015, doi: 10.3748/wjg.v21.i17.5119.

[72] S. Yim, E. Gultepe, D. H. Gracias, and M. Sitti, "Biopsy using a Magnetic Capsule Endoscope Carrying, Releasing, and Retrieving Untethered Microgrippers," *IEEE Trans. Biomed. Eng.*, vol. 61, no. 2, pp. 513–521, Feb. 2014, doi: 10.1109/TBME.2013.2283369.

[73] S. Yim and M. Sitti, "Shape-Programmable Soft Capsule Robots for Semi-Implantable Drug Delivery," *IEEE Trans. Robot.*, vol. 28, no. 5, p. 1198, 2012.

[74] S. Yim and M. Sitti, "Design and Rolling Locomotion of a Magnetically Actuated Soft Capsule Endoscope," *IEEE Trans. Robot.*, vol. 28, no. 1, pp. 183–194, Feb. 2012, doi: 10.1109/TRO.2011.2163861.

[75] E. P. Furlani, *Permanent Magnet and Electromechanical Devices: Materials, Analysis, and Applications*. Academic Press, 2001.

[76] A. J. Petruska and B. J. Nelson, "Minimum Bounds on the Number of Electromagnets Required for Remote Magnetic Manipulation," *IEEE Trans. Robot.*, vol. 31, no. 3, pp. 714–722, Jun. 2015, doi: 10.1109/TRO.2015.2424051.

[77] Y. Kotb, I. Elgamal, and M. Serry, "Shape Memory Alloy Capsule Micropump for Drug Delivery Applications," *Micromachines*, vol. 12, no. 5, Art. no. 5, May 2021, doi: 10.3390/mi12050520.

[78] "ECOFLEX_SERIES_TB.pdf." Accessed: Jul. 26, 2023. [Online]. Available: https://www.smooth-on.com/tb/files/ECOFLEX_SERIES_TB.pdf
[79] K. E. Peyer, S. Tottori, F. Qiu, L. Zhang, and B. J. Nelson, "Magnetic Helical Micromachines," *Chem. – Eur. J.*, vol. 19, no. 1, pp. 28–38, 2013, doi: 10.1002/chem.201203364.
[80] H. Lee, D. Kim, S. Kwon, and S. Park, "Magnetically Actuated Drug Delivery Helical Microrobot with Magnetic Nanoparticle Retrieval Ability," *ACS Appl. Mater. Interfaces*, vol. 13, no. 17, pp. 19633–19647, May 2021, doi: 10.1021/acsami.1c01742.
[81] H. Lee and S. Park, "Magnetically Actuated Helical Microrobot with Magnetic Nanoparticle Retrieval and Sequential Dual-Drug Release Abilities," *ACS Appl. Mater. Interfaces*, vol. 15, no. 23, pp. 27471–27485, Jun. 2023, doi: 10.1021/acsami.3c01087.
[82] U. Bozuyuk, O. Yasa, I. C. Yasa, H. Ceylan, S. Kizilel, and M. Sitti, "Light-Triggered Drug Release from 3D-Printed Magnetic Chitosan Microswimmers," *ACS Nano*, vol. 12, no. 9, pp. 9617–9625, Sep. 2018, doi: 10.1021/acsnano.8b05997.
[83] R. Wright Carlsen, M. R. Edwards, J. Zhuang, C. Pacoret, and M. Sitti, "Magnetic steering control of multi-cellular bio-hybrid microswimmers," *Lab. Chip*, vol. 14, no. 19, pp. 3850–3859, 2014, doi: 10.1039/C4LC00707G.
[84] S. Klumpp, C. T. Lefèvre, M. Bennet, and D. Faivre, "Swimming with magnets: From biological organisms to synthetic devices," *Phys. Rep.*, vol. 789, pp. 1–54, Jan. 2019, doi: 10.1016/j.physrep.2018.10.007.
[85] I. S. M. Khalil, K. Youakim, A. Sánchez, and S. Misra, "Magnetic-based motion control of sperm-shaped microrobots using weak oscillating magnetic fields," in *2014 IEEE/RSJ International Conference on Intelligent Robots and Systems*, Sep. 2014, pp. 4686–4691. doi: 10.1109/IROS.2014.6943228.
[86] I. S. M. Khalil, H. C. Dijkslag, L. Abelmann, and S. Misra, "MagnetoSperm: A microrobot that navigates using weak magnetic fields," *Appl. Phys. Lett.*, vol. 104, no. 22, p. 223701, Jun. 2014, doi: 10.1063/1.4880035.
[87] V. Magdanz *et al.*, "IRONSperm: Sperm-templated soft magnetic microrobots," *Sci. Adv.*, vol. 6, no. 28, p. eaba5855, Jul. 2020, doi: 10.1126/sciadv.aba5855.
[88] K. I. N. A. Middelhoek, V. Magdanz, L. Abelmann, and I. S. M. Khalil, "Drug-Loaded IRONSperm clusters: modeling, wireless actuation, and ultrasound imaging," *Biomed. Mater.*, vol. 17, no. 6, p. 065001, Sep. 2022, doi: 10.1088/1748-605X/ac8b4b.
[89] V. Magdanz and O. G. Schmidt, "Spermbots: potential impact for drug delivery and assisted reproductive technologies," *Expert Opin. Drug Deliv.*, vol. 11, no. 8, pp. 1125–1129, Aug. 2014, doi: 10.1517/17425247.2014.924502.
[90] H. Xu *et al.*, "Human spermbots for patient-representative 3D ovarian cancer cell treatment," *Nanoscale*, vol. 12, no. 39, pp. 20467–20481, 2020, doi: 10.1039/D0NR04488A.
[91] I. S. M. Khalil, L. Abelmann, and S. Misra, "Magnetic-Based Motion Control of Paramagnetic Microparticles With Disturbance Compensation," *IEEE Trans. Magn.*, vol. 50, no. 10, pp. 1–10, Oct. 2014, doi: 10.1109/TMAG.2014.2323940.